10.1109/ULTSYM.2015.0373

Characterization of a 3D-MEMS Piezoelectric Transducer for Portable Imaging Systems

C. Nistorica, D. Latev, D. Gardner, D. Imai
FUJIFILM Dimatix, Inc.
2250 Santa Clara CA 95050 USA

C. Daft
River Sonic Solutions
Dublin CA 94568 USA

Abstract— **This paper presents the characterization of two ultrasound transducers that were developed for two different applications. Both transducer arrays are based on a high performance PZNT film integrated in a 3D dome shaped structure, which forms the basic resonator cell of the transducer. The first transducer having wide bandwidth and low operating voltage of 20V can be implemented in a portable type of ultrasound system. The second transducer having high sensitivity, low operating voltage and a very small form factor can be implemented in miniaturized ultrasound catheters. Inter-element cross talk of less than -35dB was measured. Images of a wire target phantom were acquired using a phased array algorithm demonstrating high resolution axially and laterally.**

Keywords—PMUT; MEMS; 3D; Dome; PZNT; HIFU.

I. INTRODUCTION

Micromachined ultrasonic transducers (MUT) have multiple advantages over conventional ultrasound transducers especially for applications that require miniaturization. Developing high performance piezoelectric micro-machined ultrasound transducers (PMUT) has been hindered by the lack of high quality piezoelectric films and innovative structures that could result in high bandwidth and low voltage ultrasonic transducers. Compared to the well-known capacitive MUTs (CMUTs) [1], PMUTs have the advantage that they do not require a high voltage bias, are easier to fabricate, have better long-term reliability, lower parasitic capacitance and lower electrical impedance which is also better matched to the ultrasound systems readout electronics and coaxial cables impedance. Additionally, low fabrication costs, especially for applications requiring high volume production of small-area dice, justifies the adoption of PMUT technology in medical ultrasound imaging.

In this paper, we are presenting the characterization of a micro-machined ultrasound transducer composed of 3D dome-shaped structures with resonant frequencies that can be controlled by proper selection of the radius of the dome, hence leading to better design flexibility and larger bandwidth.

II. DESIGN

A. Structure and Materials

The material used in the fabrication of PMUTs at FUJIFILM Dimatix was a proprietary RF-sputtered, high performance and reliable niobium-doped lead zirconate titanate (PNZT) film with a very high piezoelectric coefficient ($e_{31,f}$=-23C/m2) [2]. The novel structure used was a micromachined 3D dome-shaped membrane which we have previously described in [3], and whose thickness is defined by the thickness of the PNZT film and the thin top and bottom electrodes. The PZNT film is pre-poled in the as-grown state, making a poling process unnecessary and allowing operation of the transducers without a DC bias. The thickness of the piezoelectric layer was the same for both transducers. A wide bandwidth design has been achieved by overlapping the frequency spectra of multiple resonators having various diameters similar to a high order linear filter. The monolithic ultrasonic array was defined by lithography, which has many advantages over bulk piezoelectric transducers: miniaturization capability, design flexibility, ease of integration with CMOS electronics. The transducers had a backing layer made out of TiW microspheres embedded in an epoxy. A parylene layer with a thickness of 2 µm was deposited on the surface of the transducers for electrical insulation. Both transducers were 64-elements linear arrays, however, their elevation, aperture, pitch, and number of domes per element was different. The first transducer was developed to be used in a portable ultrasound system, the design targeting higher output acoustic power and higher bandwidth. The second transducer is a 64-element array with a very narrow elevation dimension that could be integrated in a side looking intracardiac echocardiography (ICE) catheter.

The main design characteristics of the two transducers are presented in TABLE I.

TABLE I. TRANSDUCER DEFINITION

Device	***Transducer 1***	***Transducer2***
Aperture	2.5 mm	25.6 mm
Elevation	0.8 mm	8mm
Pitch	400 µm	126 µm
Elements	64	64
Domes/element	72	15

Fig. 1 presents an image of a section of Transducer 1 showing each element of the transducer being composed of multiple resonators with different resonant frequencies. Fig. 2 shows an SEM (Scanning Electron Microscope) image and an

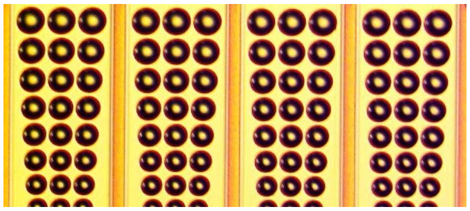

Fig. 1. Optical image of dome-shaped resonators forming the elements of the linear array.

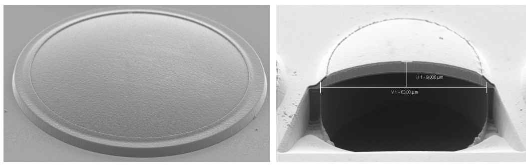

Fig. 2. SEM image and cross section image of a dome-shaped membrane.

SEM cross section image of the dome-shaped piezoelectric membrane forming each of the arrays.

III. RESULTS

A. *Sensitivity, insertion loss and beam directivity*

To measure the performance of the array, we conducted standard tests for single elements. The tests were transmit sensitivity and bandwidth, pulse-echo sensitivity and bandwidth, 50 Ω insertion loss, angular response and interelement cross coupling. The transmit measurements are based on a single element excitation using a 50ns pulse.

The main electrical characteristics of the transducers and are shown in TABLE II. The measured electrical impedance of the transducers was close to impedance values of common micro-coaxial cables usually used in Ultrasound systems, proving that with this type of transducer better matching to the imaging system can be achieved.

Fig. 3 and Fig. 4 show the typical transmit response for an element in Transducer 1 and in Transducer 2, respectively. The center frequency and -6dB fractional bandwidths for Transducer 1 and Transducer 2 were 4.7 MHz, 97% and 8.5 MHz, 47%, respectively.

TABLE II. CHARACTERIZATION RESULTS

	Transducer 1	*Transducer 2*
Center Frequency	4.7 MHz	8.5 MHz
Capacitance/ element	940 pF @ 1kHz	140pF @ 1 kHz
Impedance/ element	40 Ω @ 5MHz	80 Ω @8.5 MHz
Fractional Bandwidth (-6dB) Transmit	97%	47%
Fractional Bandwidth (-6dB) Pulse-Echo	65%	27%
Peak-to-peak pressure @ 4 mm	451kPa	390kPa

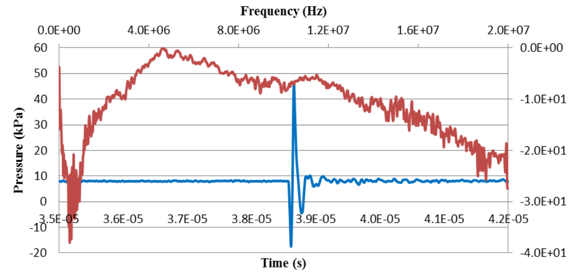

Fig. 3. Transmit impulse and frequency responses for a typical element of Tranducer1 at 6 cm in water

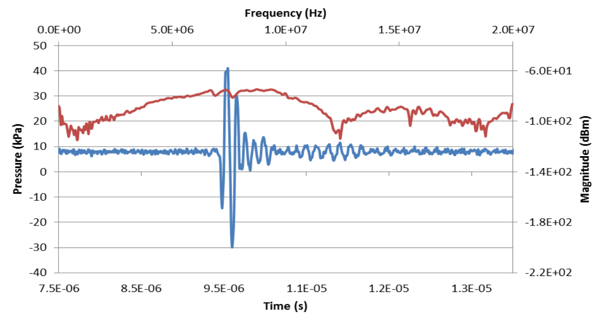

Fig. 4. Transmit impulse and frequency responses for a typical element of Transducer 2 at 2.5 cm in water.

Transducer sensitivity versus depth in water is presented in Fig. 5. The sensitivity of 85dB rel 1Pa/V for Transducer 1 shows that the PMUT array can provide output pressure that is comparable to conventional PZT ceramic transducers while having the advantage of a simpler and more flexible fabrication process. In comparison with CMUT devices [1] higher acoustic pressure can be achieved for a lower actuating voltage. The sensitivity of Transducer 2 was also high considering the very small form factor of the transducer.

Additionally, compared to other conventional reported PMUT devices [4, 5], higher transmit sensitivity and higher bandwidth has been achieved with Transducer 1 and Transducer 2.

Pulse echo measurements of single elements of the two arrays were performed by transmitting a 3 cycle burst at the center frequency of the array. For insertion-loos measurements

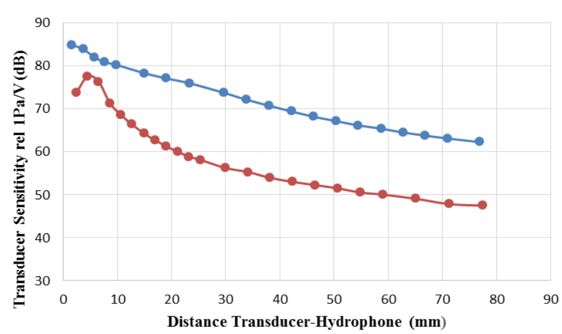

Fig. 5. Transducer Sensitivity versus depth in water

we used a Tektronix AFG3102 arbitrary function generator and an E&I RF Power amplifier with a 50 Ω output impedance to produce the desired pulse on the transmit element. The receive element was connected to the 50Ω input of the oscilloscope. The receive power across a 50 Ω load was referenced to the source power delivered to the array element and expressed in decibels. The pulse-echo sensitivity was measured off a stainless steel block in a water tank. The insertion loss was calculated using (1),

$$IL(dB) = 20 \times \log_{10}\frac{V_o}{V_i} + 0.6 + 2.2 \times 2 \times d \times f^2 \qquad (1)$$

Where V_i and V_o are input and output voltage amplitudes, respectively, d is the distance from the transducer to the stainless steel target in millimeters and f is the center frequency of the transducer. The signal loss resulted from transmission into stainless steel was compensated by 0.6dB and the signal loss due to attenuation in water was compensated by $2.2 \bullet 10^{-4}$ dB/mm•MHz^2. Diffraction losses were not taken into account. The insertion loss versus distance between transmitting element and receiving element in water is presented in Fig. 6. Comparing Transducer 2 with other small form-factor transducers used in catheters [5, 6, 7], better insertion loss and better bandwidth has been achieved with the micro-machined 3D transducer. The insertion loss for Transducers 1 is lower than some of the ultrasonic transducers manufactured using bulk PZT ceramics; however, the performance of Transducer 1 is appropriate for a portable ultrasound probe.

B. Cross Talk

The cross talk in between elements in the array was measured by transmitting on one element and receiving with another element situated at a certain distance from the transmitting element and then calculating the propagation speed of various pulses that were detected by the receiving element. Two major sources of acoustical cross talk were identified: one wave was observed to be propagating at the transducer-fluid interface at a speed almost equal to the speed of sound in water and another wave propagating in the silicon substrate. Cross talk was below -35dB, which indicated sufficient element-to-element isolation.

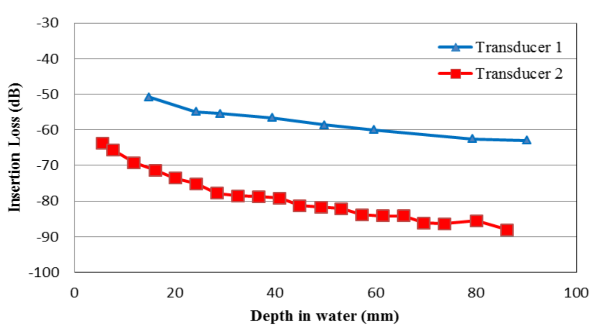

Fig. 6. Measured insertion loss for Transducer 1 and Transducer 2 versus distance between the transducer and the reflector positioned at a certain depth in water.

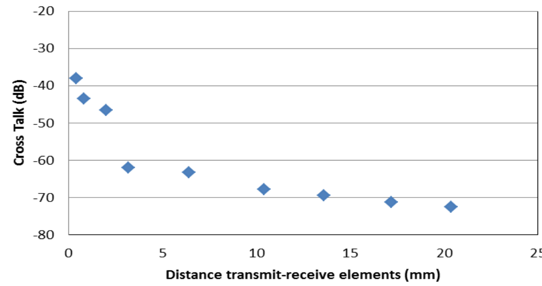

Fig. 7. Inter element cross talk.

C. Ultrasound Images

Images of a wire ultrasound phantom acquired with Transducer 1 and Transducer 2 are shown in Fig. 8 and Fig. 9, respectively. The images were acquires with a Verasonics imaging system and the transducers were driven as phased arrays in the azimuth direction. The phantom contains 100 µm diameter nylon targets spaced 1 cm axially and the wires are placed in a medium with 0.5dB/cm-MHz attenuation. The phantom also contains a resolution group at 3 cm depth that was composed of 80 µm diameter nylon wires with axial and lateral separation of 4, 3, 2, 1, 0.5 and 0.25 mm.

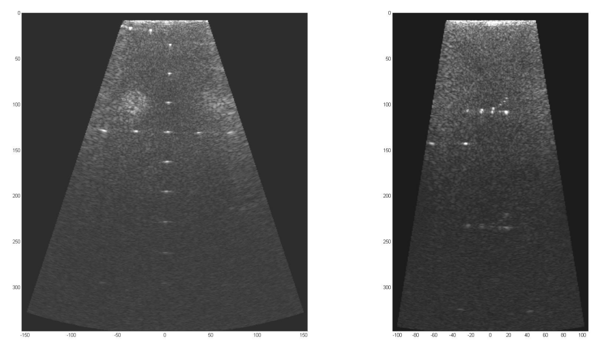

Fig. 8. Ten centimeter images of the CIRS 040GSE Ultrasound Phantom acquired with Transducer 1 operating at 20V.

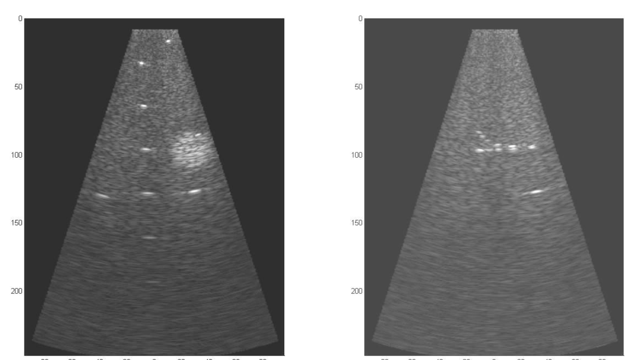

Fig. 9. Eight centimeter images of the CIRS 040GSE Ultrasound Phantom acquired with Transducer 2 operating at 20V.

The ultrasound phantom images revealed good penetration depth and resolution. Images at 10 cm depth were acquired with Transducer 1 using an operating voltage of 20V taking advantage of the good sensitivity of the transducer. Lateral resolution targets with spacing down to 1 mm were resolved at 3cm depth, while axial spacing down to 0.5 mm was resolved for both transducers. Plots of the axial and lateral line spread functions for the center wire of the phantom, placed at 3cm depth, are shown in Fig. 10 and Fig. 11. The axial and lateral resolutions for Transducer 1, measured using the full width, half-maximum of the line spread functions were 710 μm and 1066 μm, respectively. The axial and lateral resolution for Transducer 2 were 608 μm and 1810 μm, respectively. The phantom image displayed low-level sidelobes. The imaging test results show larger penetration depth for a lower voltage compared to similar arrays used in ICE catheters [8].

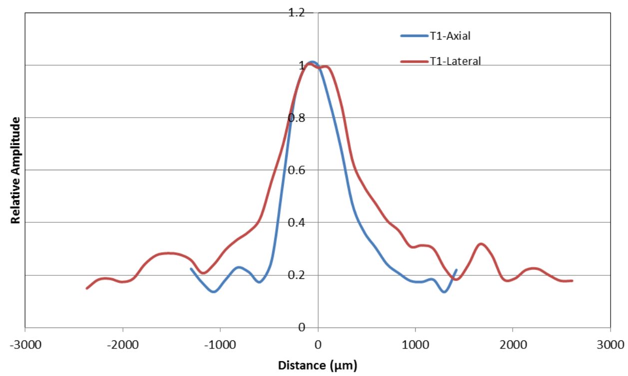

Fig. 10. Axial and lateral line spread functions for the phantom wire situated at 3 cm depth for Transducer 1.

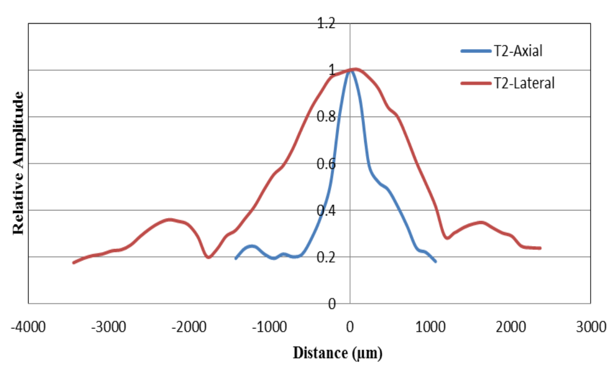

Fig. 11. Axial and lateral line spread functions for the phantom wire situated at 3 cm depth for Transducer 2.

IV. Discussion and Conclusion

We have described the characterization of two types of ultrasound transducers based on 3D piezoelectric domes technology. Ultrasound images of a wire phantom demonstrated significant penetration depth and good axial and lateral resolutions for both transducers. The results indicate that Transducer 1 can be successfully implemented in a low voltage portable imaging system. The test results for Transducer 2 prove the high potential for this miniaturized, high-sensitivity, low-voltage ultrasonic array to be developed into a side-viewing catheter and is ideal for in-vivo imaging applications such as Intracardiac Echocardiogram (ICE), endoscopy ultrasound, or phased-array HIFU ultrasound endotherapy.

Acknowledgment

Part of the work in the paper has been supported by NIH/NHLBI under grant number R4HL126364-01.

References

[1] A. S. Savoia, G. Caliano, M. PAppalardo, "A CMUT Probe for Medical Ultrasonography: From Microfabrication to System Integration", IEEE Trans. Ultrason. Ferroelect. Freq. Control, vol. 59.,pp1127- 1137, 2012.

[2] Y. Hishinuma, Y. Li, J. Birkmeyer, T. Fujii, T. Naono, and T. Arakawa, "High Performance Sputtered PZT Film for MEMS applications" Nanotech 2, 137-140 (2012).

[3] A. Hajati, D. Latev, D. Gardner, "3D MEMS piezoelectric ultrasound transducer technology", IEEE International Symposium on the Applications of Ferroelectric and Worshop on the Piezoresponse Force Microscopy", pp. 231-235, 2013.

[4] Y. Lu, D. A. Horsley, "Modeling, Fabrication, and Characterization of Piezoelectric Micromachined Ultrasonic Transducer Arrays Based on Cavity SOI Wafers", Journal of Microelectromechanical Systems, in press.

[5] D.E. Dausch, J.B. Castelucci, D.R. Chou, O.T. von Ramm, "Theory and Operation of 2-D Array piezoelectric Micromachined Transducers" IEEE Trans. Ultrason., Ferroelect., Freq. Contr., vol.55, pp 2484-2492, 2008.

[6] K. L. Gentry, S. W. Smith, "Integrated Catheter for 3D Intracardiac Echocardiography and Ultrasound Ablation", IEEE Trans. Ultrason., Ferroelect., Freq. Contr., vol.51, pp. 800-808, 2004.

[7] A miniaturized catheter 2-D array for real-time, 3-D Intracardiac Echocardiograpgy", IEEE Trans. Ultrason. Ferroelect. Freq. Control, vol.51, pp.1334-1346, 2004.

[8] D.E. Dausch, K.H. Gilchrist, J.b. Carlson, S.D.Hall, J.B. Castelluci, O.T. von Ramm," In Vivo Real-Time 3-D Intracardiac Echo Using PMUT Arrays", IEEE Trans. Ultrason., Ferroelect., Freq. Contr., vol. 61, pp. 1754-1764, 2014.